IOP Publishing | Astro Ltd
Laser Physics Letters
Laser Phys. Lett. **11** (2014) 045601 (4pp)
doi:10.1088/1612-2011/11/4/045601

Letter

Real-time optoacoustic brain microscopy with hybrid optical and acoustic resolution

Héctor Estrada[1], Jake Turner[1,2], Moritz Kneipp[1,3] and Daniel Razansky[1,3]

[1] Institute for Biological and Medical Imaging (IBMI), Helmholtz Center Munich, Ingolstädter Landstraße 1, D-85764 Neuherberg, Germany
[2] Faculty of Electrical Engineering and Information Technology, Technical University of Munich, Theresienstraße 90, D-80333 Munich, Germany
[3] Faculty of Medicine, Technical University of Munich, Ismaninger Straße 22, D-81675 Munich, Germany

E-mail: dr@tum.de

Received 25 November 2013, revised 17 January 2014
Accepted for publication 23 January 2014
Published 18 February 2014

Abstract
Conventional optoacoustic microscopy operates in two distinct modes of optical resolution, for visualization of superficial tissue layers, or acoustic resolution, intended for deep imaging in scattering tissues. Here we introduce a new microscope design with hybrid optical and acoustic resolution, which provides a smooth transition from optical resolution in superficial microscopic imaging to ultrasonic resolution when imaging at greater depths within intensely scattering tissue layers. Experimental validation of the new hybrid optoacoustic microscopy method was performed in phantoms and by means of transcranial mouse brain imaging *in vivo*.

Keywords: optoacoustic imaging, optoacoustic microscopy, *in vivo* imaging, transcranial imaging, hybrid focusing

(Some figures may appear in colour only in the online journal)

The hybrid nature of optoacoustics, which relies on the detection of ultrasonic waves generated by absorption of short-duration light pulses, has seen it become the most fascinating bioimaging tool of the last 10 years [1, 2]. In particular, optoacoustic microscopes (OAMs) take advantage of the focusing capabilities of either light [3, 4] or sound [5, 6] to form high-resolution images of optical contrast deep in scattering tissues. The two alternative strategies arise due to the need for compromise between imaging resolution and imaging depth [1]. Intuitively, light can generally be focused much more tightly than ultrasound due to its shorter wavelength range. However, diffraction-limited focusing of light generally only remains possible in the ballistic photon regime. Before reliable focusing of diffuse light in deep living tissues becomes possible, through methods such as time reversal [7], the common optical-resolution OAM strategy must rely upon scanning focused light within a large focal region of a high-frequency unfocused transducer (figure 1(a)) to provide both high lateral (optical) and axial (acoustic) resolution [4, 8]. In this design, an additional signal gain may be obtained by low numerical aperture focusing of the transducer assisted by a semi-transparent prism design [3, 9]. Nevertheless, despite the excellent sub-micron lateral resolution demonstrated in recent studies [10], the optical-resolution approaches generally experience severe limitations in terms of imaging depth due to the intense scattering of light in biological tissues, similar to conventional optical microscopy techniques [11].

From the ultrasound perspective, detection of high-resolution information is hindered by additional technology-related constraints, such as the lack of sensitive tomographic arrays at high frequencies, which forces most OAM designs to opt for using a single ultrasound detection element.

By relying on high-frequency spherically focused transducers with a high numerical aperture, acoustic-resolution

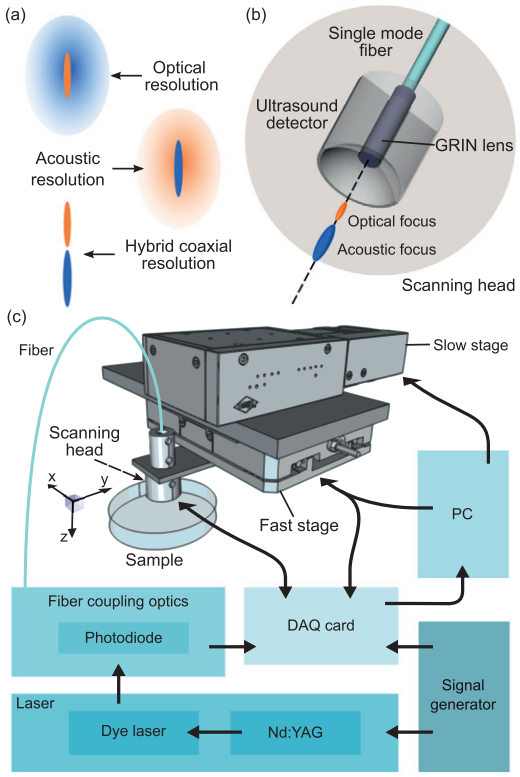

Figure 1. (a) Representation of the three optoacoustic microscopy regimes: optical resolution (orange), acoustic resolution (blue) and hybrid coaxial resolution. (b) Diagram of the scanning head of the optoacoustic microscope having two coaxial foci. (c) Schematic of the entire imaging system, including scanning mechanics, acquisition and control electronics, and the optical excitation system.

OAMs image deep tissue beyond the limitations of the ballistic regime using unfocused illumination [5, 6] (figure 1(a)). In this case, the imaging resolution is purely determined by the acoustic propagation and detection characteristics, whereas the lateral resolution is established by the focal width of the detector and the axial resolution is affected by both the detector bandwidth and ultrasound dispersion in tissues, which generally increases with frequency [12]. One major limitation arises from the fact that efficient generation of optoacoustic signals implies maximal possible confinement of the illuminating light to the sensitive area of the ultrasound detector (focal zone). This becomes challenging when attempts are made to increase imaging resolution using high numerical aperture transducers, which have to be placed close to the sample. Consequently, a suboptimal light distribution is created in the focal zone of the transducer, resulting in difficult compromises between the achievable penetration depth and the imaging speed [13, 14].

In this letter we report on an optoacoustic microscope in which a hybrid optical and acoustic-resolution approach has been implemented in order to enable real-time scanning with scalable resolution and depth (figure 1(a)). The core of the system consists of a coaxial optoacoustic head (figure 1(b)), which delivers a focused laser pulse and detects the ultrasonic pressure wave resulting from light absorption. A signal generator triggers both the data acquisition (DAQ) card (model M3i.4142, Spectrum Systementwicklung Microelectronic GmbH, Grosshansdorf, Germany) and the diode end pumped Nd:YAG Q-switched laser (model IS8II-E, Edge-Wave GmbH, Würselen, Germany) combined with a dye laser (Credo, Sirah Lasertechnik GmbH, Grevenbroich, Germany), which generate pulses of 8 ns duration at a repetition rate of up to 10 kHz, and a tunable wavelength between 575 and 605 nm for Pyrromethene 597 (figure 1(c)). The pulse is subsequently guided into a large mode area photonic crystal fiber (model LMA20, NKT Photonics A/S, Birkerd, Denmark) using standard fiber coupling optics. The output of the fiber is then focused by means of a gradient-index (GRIN) lens (Grintech GmbH, Jena, Germany). A diffraction-limited optical focus is created at a distance of approximately 6.5 mm from the lens. The generated ultrasonic responses are detected by a spherically focused piezoelectric transducer with a central frequency of 50 MHz, 67% bandwidth, 7.1 mm focal length and 6 mm active diameter (InSensor, Kvistgaard, Denmark). The fiber–lens assembly is mounted through the center of the transducer, which has a central opening 0.9 mm diameter [6]. For efficient coupling of the optoacoustically generated ultrasonic responses, the scanning head is submerged in a small tray filled with water, which contains the sample to be imaged. The tray has a circular opening in its base, sealed with a thin transparent membrane. This enables coupling of larger samples as well as *in vivo* imaging by bringing the mouse head into contact with the membrane.

In order to achieve real-time scanning, the optoacoustic head is mounted together with a fast linear piezoelectric stage (model M683; Physik Instrumente GmbH, Karlsruhe, Germany) and a slow linear stage (model LTM 60F; Owis GmbH, Staufen, Germany). With this implementation a two-dimensional scanning rate of 18 linear B-scan frames per second has been achieved for a length of 3 mm.

To monitor the oscillations in the laser pulse power, a photodiode collects around 1% of the pulse energy reflected from a beam sampler in the optical path. A personal computer (PC) controls the scanning parameters and collects data from the ultrasound transducer, the measured position of the fast stage and the photodiode readings in order to render B-scan optoacoustic images in real time.

Further control over the relative position between the scanning head and the sample is achieved using manual stages. The position of the fiber tip can be also varied in order to shift the location of the acoustic and optical foci with respect to each other. By varying the relative position of the two foci with respect to the tissue surface, we are able to flexibly adjust the functionality of the microscope. For instance, if the light illuminating the tissue surface is unfocused while the acoustic focus is located deep inside the tissue, the device effectively acts as an acoustic-resolution microscope. Conversely, if the light is focused within the first millimeter from the tissue surface, the device turns into an optical-resolution microscope. In this case, by further placing the foci immediately above one another, hybrid scanning can be implemented with optical resolution achieved in the first millimeter of tissue, followed by a slow progression into acoustic-resolution performance in deeper tissue layers (figure 1(a)).

To validate the lateral-resolution performance resulting from the optical focusing, we imaged a polyamide suture

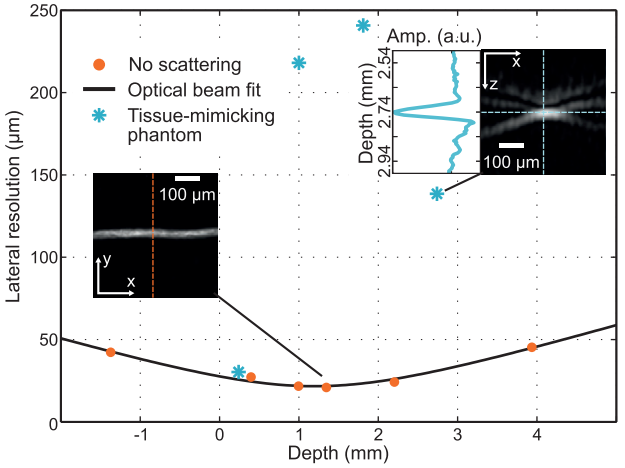

Figure 2. Optoacoustic characterization of the optical and acoustic foci using 10 μm diameter sutures. Lateral resolution of the system has been experimentally determined as a function of depth using non-scattering and tissue-mimicking suture phantoms (see legend and text for details). A quadratic fit of the non-scattering data is also shown (black curve). The insets depict the maximum amplitude projection at the optical focus and a B-scan (gray scale showing the absolute value of the measured ultrasound signal) at the acoustic focus along with the ultrasonic signal amplitude as a function of depth on its left. The surface of the tissue-mimicking phantom has been chosen as zero depth, i.e. anything located between the transducer and the phantom surface will account for negative depth.

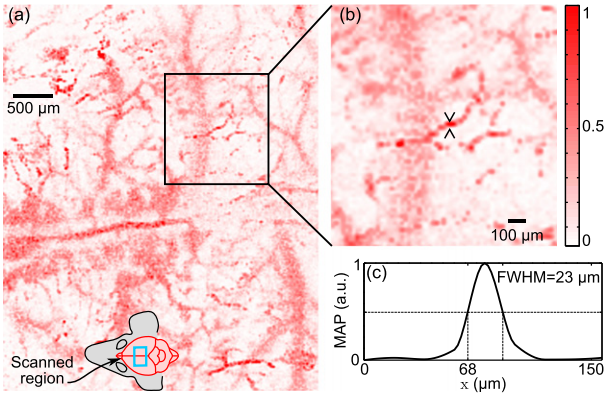

Figure 3. Optoacoustic image of the brain of a nude mouse acquired *in vivo* through an intact skull. (a) A volumetric maximal amplitude projection image acquired from an area of 4×5 mm^2, as indicated in the inset. (b) Zoom into a selected region where smaller vasculature can be identified. An inset in (a) depicts the brain region where the scan was performed. The color scale represents the normalized maximum amplitude projection. (c) Cross section of the image in (b) at the location indicated by the arrows.

of diameter $d = 10$ μm embedded in clear agar gel. The distance of the scanning head from the surface of the phantom surface was varied in order to characterize the optical focus at different positions. A typical maximum amplitude projection (MAP) optoacoustic image of the suture is presented in the left inset of figure 2. The lateral resolution is calculated from the measured full width at half maximum (FWHM) as $\sqrt{\text{FWHM}^2 - d^2}$. A Gaussian fit to the lateral cut through the image along the y-axis results in a smallest lateral resolution of 21 μm due to the optical focusing. Furthermore, using the 4σ beam width from the Gaussian fit we were able to fully characterize the optical beam as it propagates coaxially to the acoustic one, as depicted in the graph in figure 2. The orange dots showing the beam width as a function of the suture location closely resemble a Gaussian beam having a waist of $\omega_0 = 20.3$ μm at a distance $z = 6.8$ mm from the lens. Due to the low numerical aperture of the GRIN lens, the optical design possesses a focal zone of extended size with a Rayleigh length of $z_R = \pi\omega_0^2/\lambda = 2.2$ mm, where λ corresponds to the wavelength of the light.

For characterization of the acoustic-resolution performance, an additional phantom was constructed, which consisted of several sutures embedded at different depths in a scattering agar. An intralipid solution was added to the agar in order to achieve a tissue-mimicking reduced scattering coefficient of $\mu_s' = 5$ cm^{-1}. In this experiment, the optical focus was set at a depth of 1 mm from the surface of the phantom, while the acoustic focus was aligned at approximately 3 mm beneath the surface. A typical optoacoustic image, shown in the right inset of figure 2, reveals the cross-sectional profile of the suture located approximately at the focus of the transducer. A cut through the lateral direction reveals a lateral resolution of 139 μm and a suture size in the axial direction of 43 μm. Although a smaller size of the diffraction-limited (−6 dB) focal beam diameter of the transducer at its central frequency should be expected, the attained values can be considered reasonable when taking into account the final thickness of the suture and its extended length in the lateral direction, which are both convolved into the measured time profile of the signal. Furthermore, in contrast to the optical focusing part, the high numerical aperture of the ultrasonic transducer corresponds to a relatively short (−6 dB) focal zone of only about 0.34 mm. The high numerical aperture also leads to drastic degradation of the imaging resolution outside this short focal zone. Nevertheless, as was previously shown, the out-of-focus resolution can generally be restored by means of the synthetic aperture focusing technique (SAFT) [15, 16] or model-based reconstruction algorithms [17]. The blue asterisks in figure 2 denote the values for lateral resolution derived by analyzing the cross-sections of all the sutures located at different depths in the phantom. It can be seen that while the deepest and the shallowest sutures establish the acoustic and optical focusing performance well, the intermediate-resolution values at depths between 1–2 mm suffer from both intense light scattering and unfocused ultrasonic detection.

We subsequently performed transcranial imaging of a 4×5 mm^2 area of the brain of a nude mouse *in vivo*. The imaged region is schematically shown in the inset of figure 3(a). Three-dimensional (3D) image acquisition with a step size of 20 μm between adjacent pixels took about 16 s with both stages put into constant motion. An average per-pulse energy of 10 μJ at a repetition frequency of 6.1 kHz has been used in the experiment. For imaging, the scalp was partially removed while the skull remained intact. Figure 3(a) shows the maximum amplitude projection (MAP) of the raw data, i.e. no reconstruction or back-propagation algorithms were used to

obtain the images. Brain cortical vasculature is clearly visible, with hemoglobin being the main source of absorption in the illumination wavelength range employed. A zoom into the image (figure 3(b)) allows one to identify smaller capillaries in the range of 23 μm (figure 3(c)), in good agreement with the optical resolution provided by the system at tissue depths below the first millimeter.

In this letter, a new design for an optoacoustic microscope with hybrid optical and acoustic resolution has been introduced, which can extend the imaging depth of optical-resolution OAM into deeper tissue layers by means of high numerical aperture acoustic focusing. This allows for a smooth transition between optical resolution in superficial microscopic imaging to ultrasonic resolution when imaging at greater depths within intensely scattering tissues suffering from degradation of optical-resolution performance. The presented coaxial illumination and detection design facilitates optimal coupling of the excitation light into the imaged region, thus further enhancing the generated signals and accelerating image acquisition. The real-time imaging frame rate of 18 two-dimensional cross-sections per second over an imaging range of 3 mm, achieved by the current design, is mainly limited by the performance of the fast piezo stage, which can be generally improved. In summary, it is anticipated that the high temporal and spatial resolution of the system, along with its capabilities of scalable penetration into scattering tissues, will enable important new applications, e.g. in the fields of vascular diagnostics, neuroimaging, visualization of skin abnormalities and cancer research.

Acknowledgments

We gratefully acknowledge the valuable help of Erdem Başeğmez in the development of the fast scanning software. The research leading to these results has received funding from the European Research Council under grant agreement ERC-2010-StG-260991.

References

[1] Wang L V and Hu S 2012 Photoacoustic tomography: in vivo imaging from organelles to organs *Science* **335** 1458–62
[2] Ntziachristos V and Razansky D 2010 Molecular imaging by means of multispectral optoacoustic tomography (MSOT) *Chem. Rev.* **110** 2783–94
[3] Maslov K, Zhang H F, Hu S and Wang L V 2008 Optical-resolution photoacoustic microscopy for in vivo imaging of single capillaries *Opt. Lett.* **33** 929–31
[4] Xie Z, Jiao S, Zhang H F and Puliafito C A 2009 Laser-scanning optical-resolution photoacoustic microscopy *Opt. Lett.* **34** 1771–3
[5] Maslov K, Stoica G and Wang L V 2005 In vivo dark-field reflection-mode photoacoustic microscopy *Opt. Lett.* **30** 625–7
[6] Ma R, Söntges S, Shoham S, Ntziachristos V and Razansky D 2012 Fast scanning coaxial optoacoustic microscopy *Biomed. Opt. Express* **3** 1724–31
[7] Judkewitz B, Wang Y M, Horstmeyer R, Mathy A and Yang C 2013 Speckle-scale focusing in the diffusive regime with time reversal of variance-encoded light (TROVE) *Nature Photon.* **7** 300–5
[8] Chen S-L, Xie Z, Guo J L and Wang X 2013 A fiber-optic system for dual-modality photoacoustic microscopy and confocal fluorescence microscopy using miniature components *Photoacoustics* **1** 30–5
[9] Chen J, Lin R, Wang H, Meng J, Zheng H and Song L 2013 Blind-deconvolution optical-resolution photoacoustic microscopy in vivo *Opt. Express* **21** 7316–27
[10] Zhang C, Maslov K and Wang L V 2010 Subwavelength-resolution label-free photoacoustic microscopy of optical absorption *in vivo Opt. Lett.* **35** 3195–7
[11] Ntziachristos V 2010 Going deeper than microscopy: the optical imaging frontier in biology *Nature Meth.* **7** 603–14
[12] Maev R G 2008 *Acoustic Microscopy* (Weinheim: Wiley-VCH Verlag GmbH & Co.)
[13] Stein E W, Maslov K and Wang L V 2009 Noninvasive, in vivo imaging of the mouse brain using photoacoustic microscopy *J. Appl. Phys.* **105** 102027
[14] Liao L-D *et al* 2012 Transcranial imaging of functional cerebral hemodynamic changes in single blood vessels using in vivo photoacoustic microscopy *J. Cereb. Blood Flow Metab.* **32** 938–51
[15] Passmann C and Ermert H 1995 In vivo imaging of the skin in the 100 MHz region using the synthetic aperture concept *Ultrasonics Symp., 1995. Proc. 1995 IEEE* pp 1287–90
[16] Li C and Wang L V 2008 High-numerical-aperture-based virtual point detectors for photoacoustic tomography *Appl. Phys. Lett.* **93** 033902
[17] Caballero M Á A, Rosenthal A, Gateau J, Razansky D and Ntziachristos V 2012 Model-based optoacoustic imaging using focused detector scanning *Opt. Lett.* **37** 4080–2